

Geophysical Research Letters

RESEARCH LETTER

10.1029/2020GL089560

Key Points:

- Substantial intermodel spread of GM hydrological sensitivity in the CMIP5 models is found
- The intermodel spread of projected GM hydrological sensitivity could be attributed to the projected interhemispheric temperature gradient
- The intermodel spread of regional monsoon hydrological sensitivity is attributed to the projected land-ocean temperature gradient and SST pattern

Correspondence to:

J. Cao and B. Wang,
jianc@nust.edu.cn;
wangbin@hawaii.edu

Citation:

Cao, J., Wang, B., Wang, B., Zhao, H., Wang, C., & Han, Y. (2020). Sources of the intermodel spread in projected global monsoon hydrological sensitivity. *Geophysical Research Letters*, 47, e2020GL089560. <https://doi.org/10.1029/2020GL089560>

Received 27 JUN 2020

Accepted 27 AUG 2020

Accepted article online 30 AUG 2020

Sources of the Intermodel Spread in Projected Global Monsoon Hydrological Sensitivity

Jian Cao^{1,2} , Bo Wang^{1,3}, Bin Wang^{2,4} , Haikun Zhao¹ , Chao Wang^{1,2}, and Ying Han^{1,2}

¹Key Laboratory of Meteorological Disaster, Ministry of Education/Joint International Research Laboratory of Climate and Environment Change/Collaborative Innovation Center on Forecast and Evaluation of Meteorological Disasters, Nanjing University of Information Science and Technology, Nanjing, China, ²Earth System Modeling Center, Nanjing University of Information Science and Technology, Nanjing, China, ³Wenzhou Meteorological Bureau, Wenzhou, China, ⁴Department of Atmospheric Sciences, University of Hawaii at Mānoa, Honolulu, HI, USA

Abstract The projected monsoon hydrological sensitivity, namely, the precipitation change rate per kelvin of global warming, shows substantial intermodel spread among 40 Coupled Model Intercomparison Project phase 5 models. The hydrological sensitivity of the Northern Hemisphere summer monsoon is negatively correlated with that of the Southern Hemisphere summer monsoon. The intermodel spread of the Northern Hemisphere summer monsoon hydrological sensitivity is mainly attributed to the projected interhemispheric temperature gradients and the associated low-level cross-equatorial flows. The intermodel spread of the Afro-Asia summer monsoon sensitivity is rooted in the projected continent-ocean thermal gradients, while the spread of the North American monsoon sensitivity is related to the projected sea surface temperature pattern in the tropical eastern Pacific and Atlantic. These findings suggest that further constraining monsoon hydrological sensitivity requires a better projection of the warming rate between the Northern and Southern Hemispheres and between the land and ocean, and the sea surface warming pattern in the tropical eastern Pacific and Atlantic.

Plain Language Summary Global monsoon precipitation has far-reaching impacts on agriculture planning and social-economic sustainable development. Previous studies suggested that the increasing of global monsoon precipitation is sensitive to global warming rate, but the precipitation sensitivities, i.e., the precipitation change rate per kelvin of global warming, are also different among state-of-the-art coupled models. The causes of uncertainty in the monsoon precipitation sensitivity and the associated dominant physical mechanism remain elusive. Based on 40 state-of-the-art coupled climate models, we reveal that the greenhouse gas-induced interhemispheric temperature gradient causes the uncertainty of global monsoon precipitation sensitivity by changing the strengths of monsoon circulation and Hadley circulation and altering the Intertropical Convergence Zone position. Our results highlight the importance of a reliable projection of interhemispheric differential warming to the future change of global monsoon precipitation.

1. Introduction

Monsoon precipitation is the major water source for ecosystem, agriculture, and infrastructure management in the monsoon regions, where ~70% of the world's population resides. As the annual variation of insolation is a fundamental driver of the monsoon, the concept of the global monsoon (GM) is proposed to describe the strength of overall monsoon systems around the globe (Trenberth et al., 2000; Wang & Ding, 2006). The GM is the dominant mode of the annual variability of the atmosphere (Wang & Ding, 2008). It plays a central role in planetary-scale energy and water cycles (Biasutti et al., 2018; Trenberth et al., 2000; Wang et al., 2017). The GM exhibits variabilities on interannual, interdecadal, centennial, millennial, orbital, and tectonic time scales, as seen in instrumental observation and paleoproxy data (Cao et al., 2019; Liu et al., 2009; Wang et al., 2012, 2014, 2017; Zhou et al., 2008).

On the interannual time scale, GM precipitation is closely related to the El Niño–Southern Oscillation (ENSO) (Deng et al., 2018; Wang et al., 2012, 2013; Zhou et al., 2008). On the interdecadal time scale, GM precipitation, especially the Northern Hemisphere (NH) summer monsoon (NHS) precipitation, is associated with the variation of the Interdecadal Pacific Oscillation/Mega-ENSO (Wang et al., 2013) and

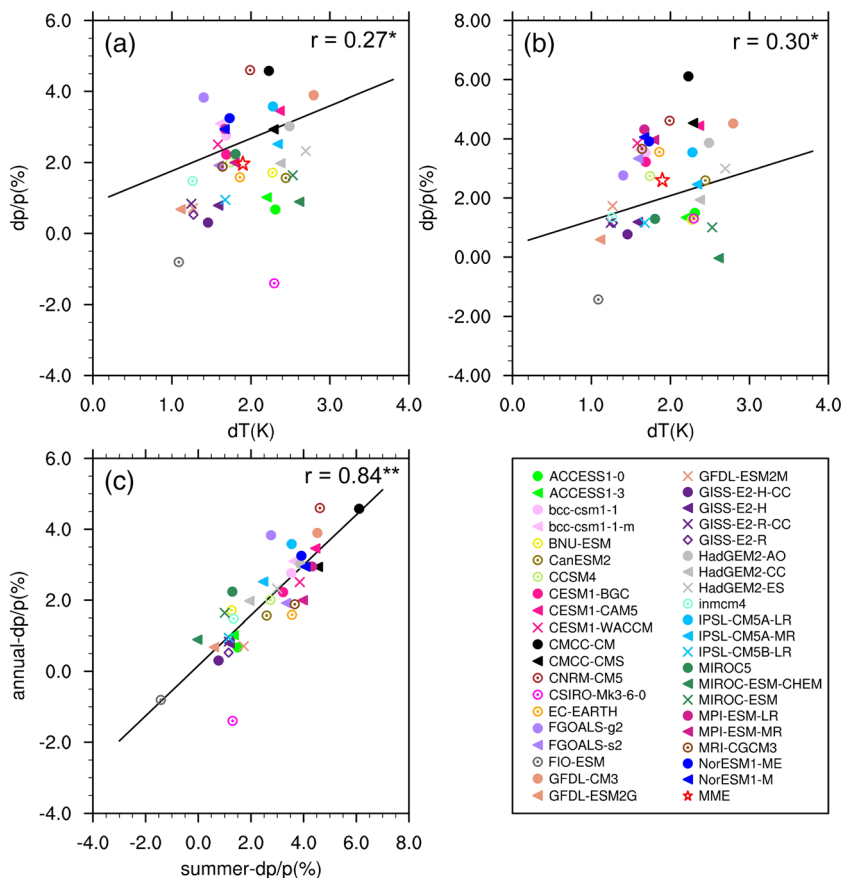


Figure 1. The relationship between the changing rates of monsoon precipitation (ordinate; %) and changes of global mean surface temperature (abscissa; K) for (a) annual mean and (b) summer mean in the 40 CMIP5 models. (c) The relationship between the changing rate of annual mean global monsoon precipitation (ordinate; %) and that of summer monsoon precipitation (abscissa; %). The changes are the differences between future (2075–2099) and historical (1979–2004) climate. The superscript “**”/“***” indicates that the correlation coefficients are significant at a 90%/95% confidence level.

Atlantic Multidecadal Oscillation (Kamae et al., 2017; Monerie et al., 2019; Wang et al., 2013) and the thermal contrast between the North Atlantic and South Indian Ocean (Wang et al., 2018). These studies further revealed that the impacts of these climate modes on GM precipitation are mainly caused by the associated changes of monsoon circulation.

Projection from the multiple Coupled Model Intercomparison Project phase 5 (CMIP5) models' ensemble mean shows an expanded GM area and enhanced GM precipitation in response to future global warming (Hsu et al., 2013; Kitoh et al., 2013; Lee & Wang, 2014). The projected enhancement of the GM precipitation amount has been attributed to the combination of two opposing effects between the weakened monsoon circulation due to stabilization of the atmosphere and the increase of atmospheric moisture content due to atmospheric warming (Hsu et al., 2012; Lee & Wang, 2014). The changes in spatial pattern of monsoon precipitation has been attributed to the shifts of tropical circulation (Chadwick et al., 2013; Held & Soden, 2006; Monerie et al., 2020; Rowell & Chadwick, 2018). Wang et al. (2020) pointed out that two greenhouse gas (GHG)-induced thermodynamic effects, i.e., the increase of specific humidity and the increase of atmospheric stability due to top-heavy heating, tend to offset each other; on the other hand, the GHG-induced horizontally differential warming results in the robust “NH-warmer-than-SH” and “land-warmer-than-ocean” patterns, as well as an “El Niño-like warming” pattern, driving circulation change (the GHG-induced dynamic effect) that plays a fundamental role in shaping the spatial patterns of the GM precipitation changes.

The increases in monsoon precipitation, however, have substantial intermodel spread (Hsu et al., 2013; Jayasankar et al., 2015; Kitoh et al., 2013; Monerie et al., 2016, 2020; Park et al., 2015; Rowell &

Chadwick, 2018). It has been argued that the considerable uncertainty of GM precipitation may be influenced by different global warming rates among the CMIP5 models (Hsu et al., 2013; Oueslati et al., 2016). However, monsoon hydrological sensitivity, defined as precipitation change rate per kelvin of global warming, is also strongly model dependent (Hsu et al., 2013; Figure 1). The underlying mechanism for the intermodel spread in monsoon hydrological sensitivity remains elusive although studies have suggested the importance of the dynamic effect (Huang et al., 2013; Kent et al., 2015; Monerie et al., 2020; Rowell & Chadwick, 2018; Xie et al., 2015). Understanding what constrains the monsoon hydrological sensitivity is useful for increasing the confidence in projected precipitation change that guides water resource management.

Here we use a large ensemble of the CMIP5 models to identify the source of the intermodel spread of GM hydrological sensitivity and investigate the mechanism responsible for this spread. The models and data are described in section 2, the inter-model spread of GM hydrological sensitivity is presented in section 3, and the underlying cause is detected in section 4. We draw conclusions in section 5.

2. Data and Method

The average of the monthly Global Precipitation Climatology Project (Huffman et al., 2009) and Climate Prediction Center Merged Analysis of Precipitation data (Xie & Arkin, 1997) from 1979 to 2003 is used as the observation to define the GM domain (Wang et al., 2012). In this paper, the GM domain refers to all the areas where the summer-minus-winter precipitation exceeds 2 mm day^{-1} , and the total summer precipitation accounts for over 55% of the annual amount (Liu et al., 2009). Here May–September is defined as the NH summer and the Southern Hemisphere (SH) winter, while November–March is regarded as the NH winter and the SH summer. In this study, the monsoon precipitation is the average of the observed GM domain.

To investigate the intermodel spread of projected GM change, the historical and Representative Concentration Pathways 4.5 (RCP4.5) simulations from 40 CMIP5 models are used. The RCP4.5 scenario assumes the radiative forcing stabilized at $\sim 4.5 \text{ W m}^{-2}$ after 2100 (Moss et al., 2010). The first realizations (realization 1) of historical and RCP4.5 experiments in the 40 CMIP5 models are employed. The changes in global mean surface temperature (GMST) and GM precipitation are the differences between future (2075–2099) and historical (1979–2004) climate. The model fields are interpolated onto a $1^\circ \text{ latitude} \times 1^\circ \text{ longitude}$ grid for easy comparison among the models. We did a sensitivity test for interpolating the field onto a $2.5^\circ \text{ latitude} \times 2.5^\circ \text{ longitude}$ grid, which yields similar results (not shown).

3. Intermodel Spread of Monsoon Hydrological Sensitivity

Figure 1 shows the changing rate of annual mean GM precipitation and summer monsoon precipitation against the historical (1979–2004) climatology. The multimodel ensemble means (MMMs) of annual mean and summer mean GM precipitation are increased by 2.0% and 2.6% (Figures 1a and 1b), respectively. Both annual mean GM precipitation and summer mean GM precipitation show large intermodel spread among the CMIP5 models, ranging from -1.4% to 4.6% and from -1.4% to 6.1% (Figures 1a and 1b), respectively. The intermodel spread of the annual mean GM precipitation is closely related to that of the summer mean GM precipitation ($r = 0.84$, $p < 0.01$), indicating the intermodel spread is mainly during the summer season (Figure 1c). Note that models from the same modeling center generally show small difference in projected annual mean and summer mean GM precipitation changes (i.e., Australian Community Climate and Earth System Simulator [ACCESS], Beijing Climate Center [BCC], Community Earth System Model [CESM], Goddard Institute for Space Studies [GISS], Max Planck Institute [MPI], and Norwegian Earth System Model [NorESM]) (Knutti et al., 2010, 2013; Monerie et al., 2016). The magnitude of precipitation change may be modulated by the magnitude of GMST anomalies (GMSTA) (e.g., Li et al., 2013). We calculated the correlation coefficients between the changing rate of annual mean (summer mean) GM precipitation and the GMSTA; the correlation coefficient 0.27 (0.3) is only significant at the 90% confidence level, suggesting that the intermodel spread of GM precipitation cannot be well explained by the intermodel spread of GMSTA.

We then computed the ratio of change of GM precipitation to GMSTA, referred to as monsoon hydrological sensitivity (Fläschner et al., 2016; Li et al., 2013); it describes monsoon precipitation change per unit

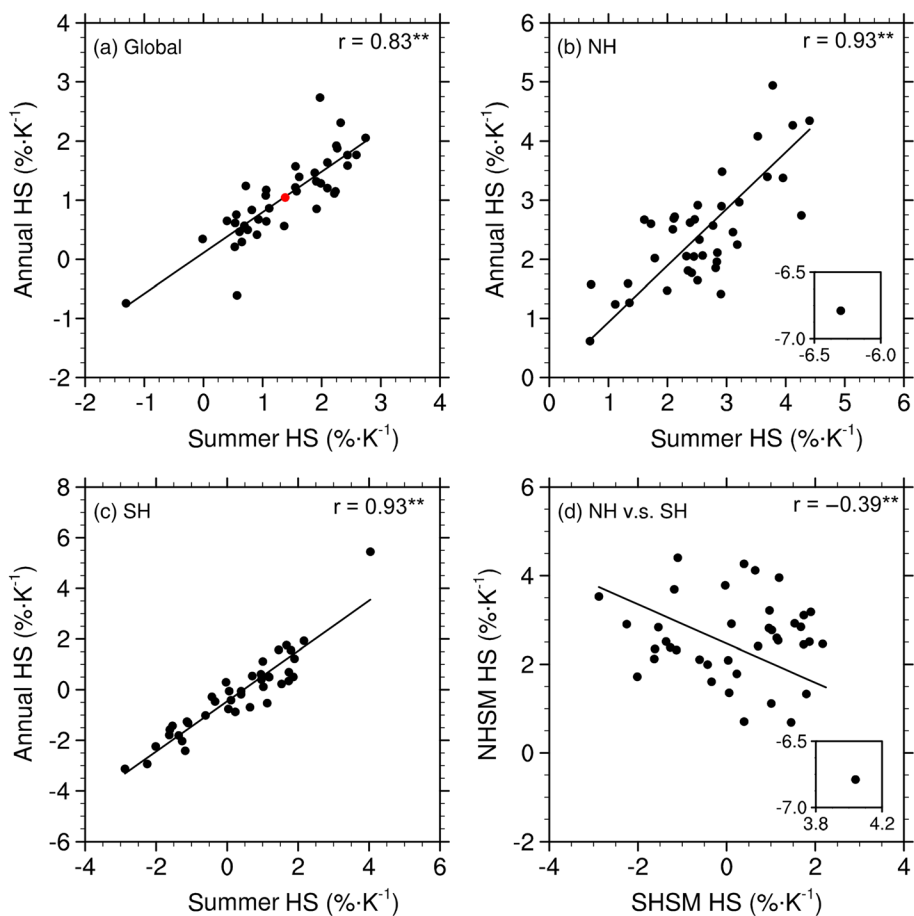


Figure 2. The changes of annual mean monsoon hydrological sensitivity ($\% \text{ K}^{-1}$) and summer monsoon hydrological sensitivity ($\% \text{ K}^{-1}$) over (a) the globe, (b) the Northern Hemisphere, and (c) the Southern Hemisphere in the 40 CMIP5 models. (d) The relationship between the NHSW hydrological sensitivity and SHSM hydrological sensitivity in the 40 CMIP5 models. The red dot in (a) indicates the multimodel ensemble mean. The superscript “**” indicates that the correlation coefficients are significant at a 95% confidence level.

of GMST change. Figure 2 shows the relationship between the annual mean monsoon hydrological sensitivity and summer monsoon hydrological sensitivity over the globe, NH, and SH. The monsoon hydrological sensitivity shows substantial differences among the CMIP5 models over the globe, NH, and SH (Figures 2a–2c), indicating that these models simulated great differences in monsoon precipitation changes under the same level of global warming. Besides, the annual mean of monsoon hydrological sensitivity is highly dependent on its summer season with the correlation coefficients of 0.83 ($p < 0.01$), 0.93 ($p < 0.01$), and 0.93 ($p < 0.01$) over the globe, NH, and SH, respectively, suggesting the dominant role of intermodel spread of summer monsoon hydrological sensitivity (Figure 2).

The projected MMM of summer monsoon precipitation increases by $\sim 1.5\% \text{ K}^{-1}$ global warming (Figure 2a). It is dominated by the NHSW hydrological cycle change ($2.4\% \text{ K}^{-1}$) (Figure 2b). In contrast, the SH summer monsoon (SHSM) precipitation only increases by $0.26\% \text{ K}^{-1}$ (Figure 2c). However, the large intermodel spread of summer monsoon hydrological sensitivity exists over both the NH and the SH, with the standard deviation being $1.7\% \text{ K}^{-1}$ and $1.5\% \text{ K}^{-1}$, respectively. The NHSW hydrological sensitivity is significantly negatively correlated with the SHSM hydrological sensitivity (Figure 2d), indicating an antiphase response of summer monsoon precipitation change over the hemispheres. It also suggests that a similar physical mechanism may be responsible for the intermodel spread of NHSW and SHSM hydrological sensitivity.

4. Mechanism

4.1. Relationship Between Monsoon Hydrological Sensitivity and Large-Scale Temperature and Circulation

Previous studies revealed that the GM is driven by the changes in large-scale temperature pattern and its associated circulation (Deng et al., 2018; Kamae et al., 2017; Wang et al., 2012, 2013; Zhou et al., 2008). To understand the mechanism behind the intermodel spread of summer monsoon hydrological sensitivity, we regressed the GMSTA-scaled anomalies of 2-m temperature over land, sea surface temperature (SST) over the ocean, and the circulations to the hydrological sensitivity across the CMIP5 models (Figure 3). The regressed surface temperature is characterized by a pattern of warm NH and cool SH. High hydrological sensitivity is associated with a warm NH but a cool SH, which suggests that the hemispheric thermal contrast plays a critical role in controlling the intermodel spread of hydrological sensitivity (Figure 3a). Meanwhile, the low-level cross-equatorial flow is enhanced in the models with high hydrological sensitivity. The NH-SH thermal contrast results in an anomalous cross-equatorial flow, which is prominent over the northern Indian Ocean, Bay of Bengal, South China Sea, and North Atlantic Ocean (Figure 3a). The enhanced cross-equatorial flow transports more moisture from the SH to NH monsoon regions (not shown). In the upper troposphere, there is a clear southward cross-equatorial flow associated with the low-level northward cross-equatorial flow, and the vertical shear of zonal wind is enhanced (Figure 3b). This circulation pattern would enhance the convergence over the NH monsoon region. Thus, more monsoon precipitation is produced in the models, which project large interhemispheric thermal contrasts. Those are the models with higher monsoon hydrological sensitivity.

The SHSM hydrological sensitivity-regressed temperature and circulation patterns are similar with that regressed by the NHSM hydrological sensitivity, but with reversed polarity (Figure 3c). It indicates that a similar mechanism operates for the intermodel spread of SHSM hydrological sensitivity. The negative correlation of summer monsoon hydrological sensitivity between the NH and the SH is associated with the large-scale temperature contrasts between hemispheres (Figures 3a and 3c). To summarize, the interhemispheric thermal contrast is of vital importance in controlling both NHSM and SHSM hydrological sensitivity.

4.2. Thermal Contrast Driving the Strength of Circulation and Movement of the ITCZ

Wang et al. (2013) suggested that the change of the NHSM system is associated with the changes of NHSM circulation and boreal summer Hadley circulation. Figure 4 shows the relationship between hydrological sensitivity and the GMSTA-scaled interhemispheric temperature difference (ITD) index among the 40 CMIP5 models and the relationship between the ITD and circulation indices (including the NHSM circulation index, the Hadley circulation index, and the Intertropical Convergence Zone (ITCZ) movement during the boreal summer). SST is used to calculate the ITD index because it is recognized to be the driving force of monsoon precipitation change (Kamae et al., 2017; Wang et al., 2012, 2013; Zhou et al., 2008). The ITD index is defined as the GMSTA-scaled SST difference between (0°N to 40°N , 0° to 360°) and (40°S to 0° , 0° to 360°). And the ITCZ movement can be reflected by the ITD-induced across-equatorial heat transport (Donohoe et al., 2013; Kang et al., 2008; Philander et al., 1996; Schneider et al., 2014; Xiang et al., 2018). The NHSM circulation is represented by the GMSTA-scaled vertical shear of zonal wind between 850 and 200 hPa over the region of 0°N to 20°N , 120°W to 120°E (Wang et al., 2013). The Hadley circulation is measured by the GMSTA-scaled zonally averaged meridional mass stream function between 100 and 1,000 hPa over the band of 30°S to 10°N (Wang et al., 2013), and the latitude of precipitation centroid is used as the ITCZ location (Donohoe et al., 2013; Frierson & Hwang, 2012).

The intermodel correlation of hydrological sensitivity and the ITD index is 0.77, exceeding the 99% confidence level (Figure 4a). It suggests that the ITD likely influences the NHSM hydrological sensitivity. We further examine how the ITD affects NHSM hydrological sensitivity via changes in the NHSM circulation, Hadley circulation, and the ITCZ. The results show robust relationships of the ITD index with the NHSM circulation index ($r = 0.52$, $p < 0.01$), the Hadley circulation index ($r = -0.86$, $p < 0.01$), and the northward movement of the ITCZ location ($r = 0.59$, $p < 0.01$) (Figures 4b–4d). In other words, the larger ITD enhances the NHSM circulation and Hadley circulation, leading to enhancement of moisture convergence over the monsoon regions. The models with large ITD, which is associated with large monsoon hydrological sensitivity, simulate larger vertical zonal wind shear. An observational study suggested that an enhanced vertical wind shear between 850 and 200 hPa is a good indication of a strong monsoon heating (Webster &

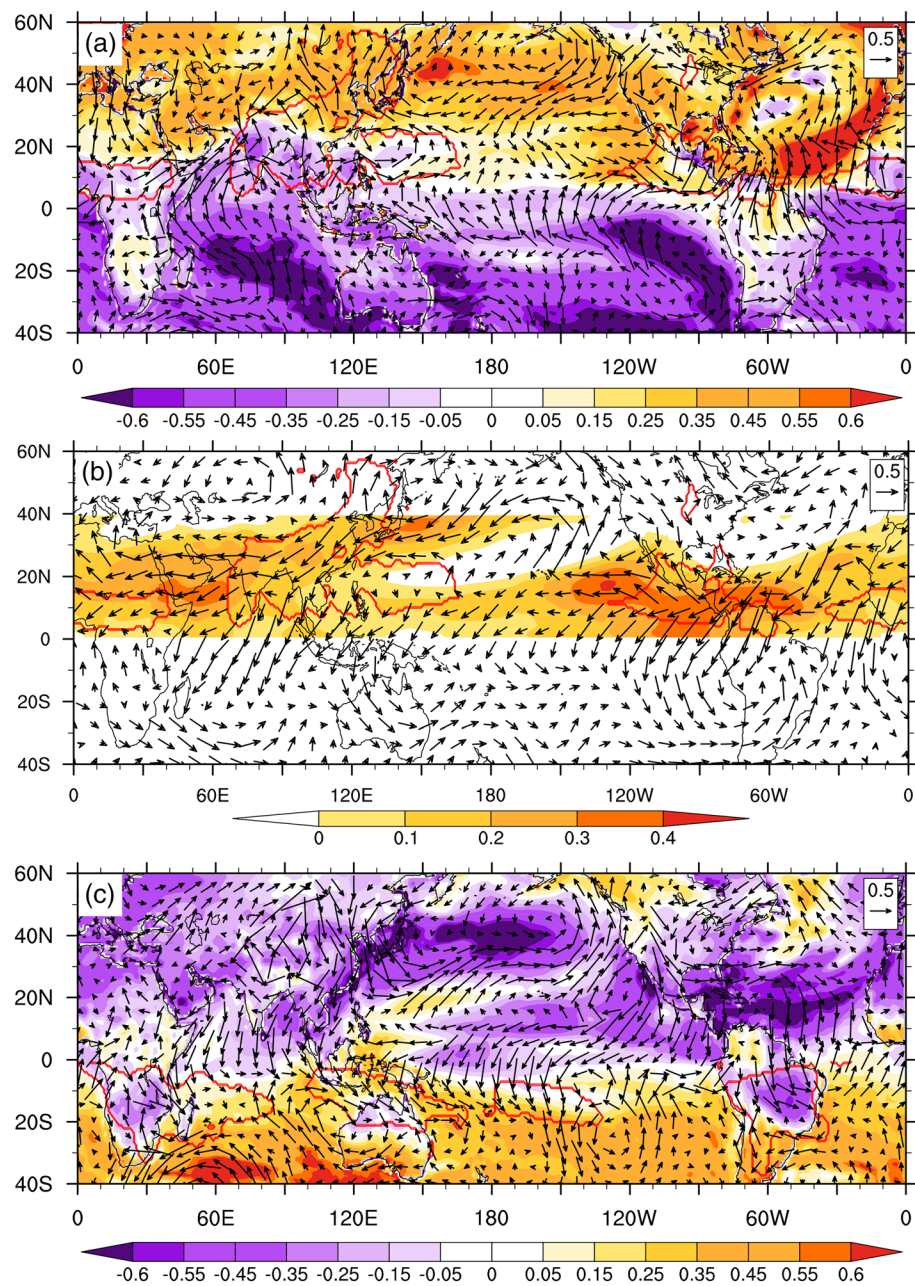


Figure 3. (a) GMSTA-scaled boreal summer surface temperature anomalies (2-m air temperature anomalies over land, SST over ocean; shading; K) and 850-hPa wind ($\text{m s}^{-1} \text{K}^{-1}$) anomalies regressed to NHSM hydrological sensitivity ($\% \text{K}^{-1}$). (b) GMSTA-scaled boreal summer 200-hPa wind ($\text{m s}^{-1} \text{K}^{-1}$) and vertical shear of zonal wind (only shown $0\text{--}40^\circ\text{N}$, shaded; $\text{m s}^{-1} \text{K}^{-1}$) anomalies regressed to NHSM hydrological sensitivity ($\% \text{K}^{-1}$). (c) GMSTA-scaled austral summer averaged surface temperature anomalies (2-m air temperature anomalies over land, SST over ocean; shading; K) and 850-hPa wind ($\text{m s}^{-1} \text{K}^{-1}$) anomalies regressed to NHSM hydrological sensitivity ($\% \text{K}^{-1}$). The anomalies are the differences between future (2075–2099) and historical (1979–2004) climate. The red lines outline the NH monsoon domain in (a) and (b) and the SH monsoon domain in (c).

Yang, 1992). The vertical shear of zonal wind can be regarded as the low-frequency baroclinic Rossby wave response to the monsoon heating (Webster & Yang, 1992).

During the boreal summer, the upward branch of the Hadley circulation is located in the NH, and an enhanced Hadley circulation is accompanied by a northward cross-equatorial flow in the lower troposphere and strengthened ascending motion between 5°N and 25°N . The NH monsoon domain largely overlaps this

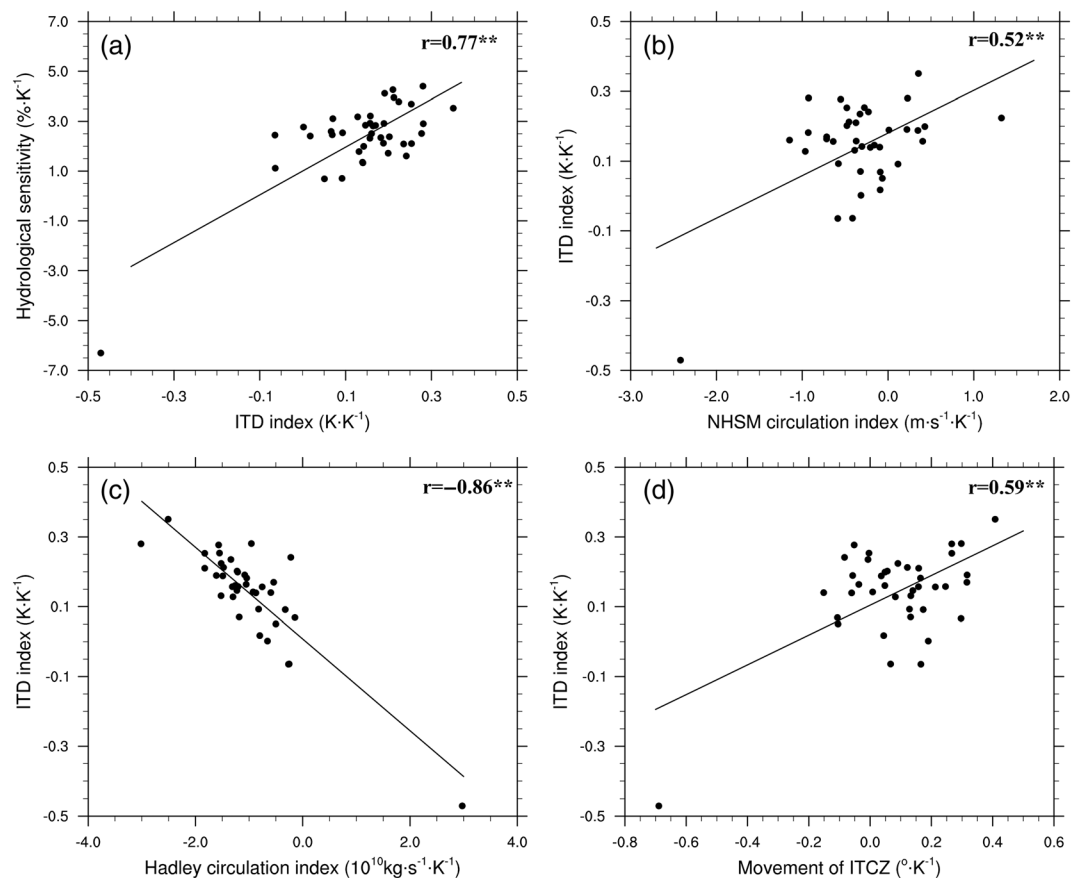


Figure 4. The relationship between NH summer monsoon hydrological sensitivity ($\% \text{ K}^{-1}$) and GMSTA-scaled (a) interhemispheric thermal contrast index (K K^{-1}), (b) NHSM circulation index ($\text{m s}^{-1} \text{ K}^{-1}$), (c) Hadley circulation index ($10^{10} \text{ kg s}^{-1} \text{ K}^{-1}$), and (d) ITCZ movement ($^{\circ} \text{ K}^{-1}$) during May–September. The negative Hadley circulation index means an enhanced ascending motion over the NH and descending motion over the SH. The indices are obtained from the differences between future (2075–2099) and historical (1979–2004) climate. The superscript “**” indicates that the correlation coefficients are significant at a 95% confidence level.

band; thus, the summer monsoon precipitation would be increased when the Hadley circulation is enhanced (Figure 4c). That is how the ITD modulates monsoon hydrologic sensitivity by changing the strength of the Hadley circulation (Figure 4c).

The monsoon has a close relationship with the ITCZ (Biasutti et al., 2018; Wang et al., 2014, 2017). Figure 4d shows the relationship between the ITD and the ITCZ movement among the 40 CMIP5 models. The models would project the northward shift of the ITCZ when the projected ITD is larger, because it generates anomalous heat transport across the equator (Donohoe et al., 2013; Kang et al., 2008; Schneider et al., 2014; Xiang et al., 2018). The associated meridional shift of the Hadley circulation further enhances the monsoon precipitation. Therefore, the NHSM precipitation will be enhanced when the boreal summer ITCZ shifts northward.

4.3. Regional Monsoon Hydrological Sensitivity

At the regional scale, the monsoon hydrological sensitivity may also be driven by adjacent environmental conditions. The North American monsoon hydrological sensitivity is highly correlated with the tropical North Atlantic (TNA; 10–25°N, 80–20°W)-southeastern Pacific Ocean (SPO; 40–15°S, 150–70°W) index (Figure 5a). The TNA-SPO index is defined as the GMSTA-scaled SST difference between the TNA and the SPO. It is suggested that a low-value TNA-SPO index will weaken the North American monsoon precipitation, while a large positive-value TNA-SPO index will enhance the North American monsoon precipitation.

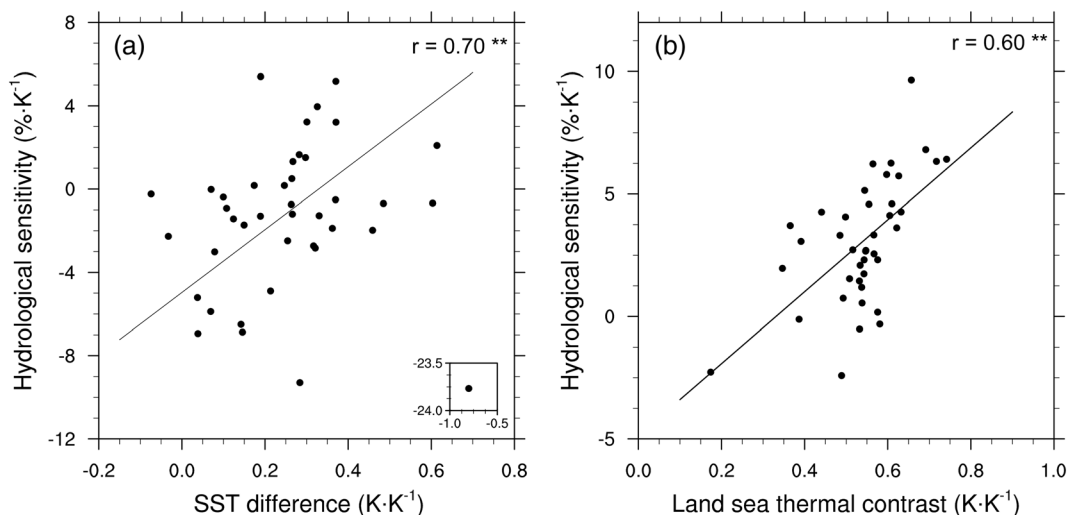


Figure 5. (a) Relationship between North American summer monsoon hydrological sensitivity and GMSTA-scaled SST difference between the tropical North Atlantic Ocean ($10\text{--}25^\circ\text{N}$, $80\text{--}20^\circ\text{W}$) and southeastern Pacific Ocean ($40\text{--}15^\circ\text{S}$, $150\text{--}70^\circ\text{W}$). (b) The relationship between Afro-Asian summer monsoon hydrological sensitivity and scaled land-sea thermal contrast. The scaled land-sea thermal contrast is defined as the surface air temperature difference between NH land (except North American continent) and the global ocean (40°S to 60°N) scaled by the GMSTA. The indices are obtained from the differences between future (2075–2099) and historical (1979–2004) climate. The superscript “ ** ” indicates that the correlation coefficients are significant at a 95% confidence level.

Previous studies suggested that the land-sea thermal contrast is one of the formation mechanisms of the Asian monsoon (e.g., Webster, 1987). Figure 5b shows the relationship between the land-sea thermal contrast index and Afro-Asian monsoon hydrological sensitivity. Here the land-sea thermal contrast index is the GMSTA-scaled temperature difference between the NH land (except the North American continent) and global ocean (40°S to 60°N). The scaled land-sea thermal contrast is closely related to the Afro-Asian monsoon hydrological sensitivity. The enlarged land-sea thermal contrast can increase the sea level pressure gradients between the continent and its adjacent ocean, thus enhancing the monsoon circulations. It dynamically drives a more vigorous monsoon hydrological cycle.

5. Conclusions

Previous studies on the future change of GM or its regional features are usually based on the MMM results (Hsu et al., 2013; Jayasankar et al., 2015; Kitoh et al., 2013; Monerie et al., 2016; Park et al., 2015). The MMM of CMIP5 models projects an increase in GM precipitation under future global warming, while the uncertainty of quantitative precipitation increase remains large in the CMIP5 models. We investigated the cause of the intermodel spread of GM hydrological sensitivity, which is defined as monsoon precipitation change scaled to 1 K global warming, in 40 CMIP5 models under the RCP4.5 scenario. The intermodel spread of GM hydrological sensitivity is tightly related to the summer monsoon hydrological sensitivity. The NHSMS hydrological sensitivity is robustly negatively correlated to the SHSM hydrological sensitivity, suggesting a similar physical mechanism for the intermodel spread of summer monsoon hydrological sensitivity for both the NH and the SH.

Over the NH, the high monsoon hydrological sensitivity is accompanied by the interhemispheric thermal contrast, i.e., a warm NH and a cool SH. This supports the assertion that the NH monsoon precipitation will increase significantly more than will the SH counterpart due to the increase in temperature difference between the NH and the SH (Lee & Wang, 2014). On the one hand, the interhemispheric thermal contrast is associated with an enhanced low-level cross-equatorial flow over the Indian Ocean, the western Pacific Ocean, and the Atlantic Ocean. It increases the moisture convergence of the Afro-Asian summer monsoon and the updraft of the Hadley circulation; meanwhile, the enhanced downward of the Hadley circulation would reduce the SH winter monsoon precipitation. On the other hand, the spread in the change of thermal contrast over the eastern hemisphere causes the uncertainties of the Afro-Asian monsoon precipitation

(Figure 5), and the uncertainties in the projected tropical eastern Pacific and Atlantic SST causes the uncertainties in the central North American monsoon precipitation. The interhemispheric thermal contrast mechanism is also valid during the austral summer over the SH. The high SHSM hydrological sensitivity is dominated by a warm SH and a cool NH. The interhemispheric temperature gradient enhances southward moisture transport.

Results of this study suggest that the intermodel spread of monsoon hydrological sensitivity is primarily driven by the GHG-induced surface temperature patterns and the corresponding monsoon circulation change among the CMIP5 models. Further restraining the monsoon hydrological cycle requires a better intermodel consistency in the projection of the interhemispheric temperature gradient, land-ocean temperature gradient, and the tropical SST pattern.

Data Availability Statement

The CMIP5 data used in this study are freely available through the Earth System Grid Federation (<https://esgf-node.llnl.gov>).

Acknowledgments

Comments from two anonymous reviewers are deeply appreciated. This work is supported by the Natural Science Foundation of China of Jiangsu Province (BK20180812 and BK20170941), the National Key R&D Program of China (2017YFA0603801), the Startup Foundation for Introducing Talent of NUIST (Grant 2018r063), and the National Natural Science Foundation of China (41730961 and 41922033). The authors acknowledge the World Climate Research Programme's Working Group on Coupled Modelling, which is responsible for the CMIP, and we thank the climate modeling groups for producing and making available their model output. This is Publication No. 1471 of the IPRC, Publication No. 11133 of the SOEST, and Publication No. 323 of the Earth System Modeling Center (ESMC).

References

- Biasutti, M., Voigt, A., Boos, W. R., Braconnot, P., Hargreaves, J. C., Harrison, S. P., et al. (2018). Global energetics and local physics as drivers of past, present and future monsoons. *Nature Geoscience*, 11(6), 392–400. <https://doi.org/10.1038/s41561-018-0137-1>
- Cao, J., Wang, B., & Ma, L. (2019). Attribution of global monsoon response to the last glacial maximum forcings. *Journal of Climate*, 32(19), 6589–6605. <https://doi.org/10.1175/JCLI-D-18-0871.1>
- Chadwick, R., Boulle, I., & Martin, G. (2013). Spatial patterns of precipitation change in CMIP5: Why the rich do not get richer in the tropics. *Journal of Climate*, 26(11), 3803–3822. <https://doi.org/10.1175/JCLI-D-12-00543.1>
- Deng, K., Yang, S., Ting, M., Tan, Y., & He, S. (2018). Global monsoon precipitation: Trends, leading modes, and associated drought and heat wave in the Northern Hemisphere. *Journal of Climate*, 31(17), 6947–6966. <https://doi.org/10.1175/JCLI-D-17-0569.1>
- Donohoe, A., Marshall, J., Ferreira, D., & Mcgee, D. (2013). The relationship between ITCZ location and cross-equatorial atmospheric heat transport: From the seasonal cycle to the Last Glacial Maximum. *Journal of Climate*, 26(11), 3597–3618. <https://doi.org/10.1175/JCLI-D-12-00467.1>
- Flaschner, D., Mauritsen, T., & Stevens, B. (2016). Understanding the intermodel spread in global mean hydrological sensitivity. *Journal of Climate*, 29(2), 801–817. <https://doi.org/10.1175/JCLI-D-15-0351.1>
- Frierson, D., & Hwang, Y. (2012). Extratropical influence on ITCZ shifts in slab ocean simulations of global warming. *Journal of Climate*, 25(2), 720–733. <https://doi.org/10.1175/JCLI-D-11-00116.1>
- Held, I. M., & Soden, B. J. (2006). Robust responses of the hydrological cycle to global warming. *Journal of Climate*, 19(21), 5686–5699. <https://doi.org/10.1175/jcli3990.1>
- Hsu, P. C., Li, T., Luo, J. J., Murakami, H., Kitoh, A., & Zhao, M. (2012). Increase of global monsoon area and precipitation under global warming: A robust signal? *Geophysical Research Letters*, 39, L06701. <https://doi.org/10.1029/2012GL051037>
- Hsu, P. C., Li, T., Murakami, H., & Kitoh, A. (2013). Future change of the global monsoon revealed from 19 CMIP5 models. *Journal of Geophysical Research: Atmospheres*, 118, 1247–1260. <https://doi.org/10.1002/jgrd.50145>
- Huang, D.-Q., Zhu, J., Zhang, Y.-C., & Huang, A.-N. (2013). Uncertainties on the simulated summer precipitation over Eastern China from the CMIP5 models. *Journal of Geophysical Research: Atmospheres*, 118, 9035–9047. <https://doi.org/10.1002/jgrd.50695>
- Huffman, G. J., Adler, R. F., Bolvin, D. T., & Gu, G. (2009). Improving the global precipitation record: GPCP version 2.1. *Geophysical Research Letters*, 36, L17808. <https://doi.org/10.1029/2009GL040000>
- Jayasankar, C. B., Surendran, S., & Rajendran, K. (2015). Robust signals of future projections of Indian summer monsoon rainfall by IPCC AR5 climate models: Role of seasonal cycle and interannual variability. *Geophysical Research Letters*, 42, 3513–3520. <https://doi.org/10.1002/2015GL063659>
- Kamae, Y., Li, X., Xie, S. P., & Ueda, H. (2017). Atlantic effects on recent decadal trends in global monsoon. *Climate Dynamics*, 49(9–10), 3443–3455. <https://doi.org/10.1007/s00382-017-3522-3>
- Kang, S. M., Held, I. M., Frierson, D. M. W., & Zhao, M. (2008). The response of the ITCZ to the extratropical thermal forcing: Idealized slab-ocean experiments with a GCM. *Journal of Climate*, 21(14), 3521–3532. <https://doi.org/10.1175/2007JCLI2146.1>
- Kent, C., Chadwick, R., & Rowell, D. (2015). Understanding uncertainties in future projections of seasonal tropical precipitation. *Journal of Climate*, 28(11), 4390–4413. <https://doi.org/10.1175/JCLI-D-14-00613.1>
- Kitoh, A., Endo, H., Krishna Kumar, K., Cavalcanti, I. F. A., Goswami, P., & Zhou, T. (2013). Monsoons in a changing world: A regional perspective in a global context. *Journal of Geophysical Research: Atmospheres*, 118, 3053–3065. <https://doi.org/10.1002/jgrd.50258>
- Knutti, R., Ringer, M., Tebaldi, C., Cermak, J., & Meehl, G. A. (2010). Challenges in combining projections from multiple climate models. *Journal of Climate*, 23(10), 2739–2758. <https://doi.org/10.1175/2009JCLI3361.1>
- Knutti, R., Masson, D., & Gettelman, A. (2013). Climate model genealogy: Generation CMIP5 and how we got there. *Geophysical Research Letters*, 40, 1194–1199. <https://doi.org/10.1002/grl.50256>
- Lee, J. Y., & Wang, B. (2014). Future change of global monsoon in the CMIP5. *Climate Dynamics*, 42(1–2), 101–119. <https://doi.org/10.1007/s00382-012-1564-0>
- Li, G., Harrison, S. P., Bartlein, P. J., Izumi, K., & Colin Prentice, I. (2013). Precipitation scaling with temperature in warm and cold climates: An analysis of CMIP5 simulations. *Geophysical Research Letters*, 40, 4018–4024. <https://doi.org/10.1002/grl.50730>
- Liu, J., Wang, B., Ding, Q., Kuang, X., Soon, W., & Zorita, E. (2009). Centennial variations of the global monsoon precipitation in the last millennium: Results from ECHO-G model. *Journal of Climate*, 22(9), 2356–2371. <https://doi.org/10.1175/2008JCLI2353.1>
- Monerie, P. A., Robson, J., Dong, B., Hodson, D. L. R., & Klingaman, N. P. (2019). Effect of the Atlantic multidecadal variability on the global monsoon. *Geophysical Research Letters*, 46, 1765–1775. <https://doi.org/10.1029/2018GL080903>

- Monerie, P.-A., Sanchez-Gomez, E., & Boé, J. (2016). On the range of future Sahel precipitation projections and the selection of a sub-sample of CMIP5 models for impact studies. *Climate Dynamics*, 48(7-8), 2751–2770. <https://doi.org/10.1007/s00382-016-3236-y>
- Monerie, P.-A., Wainwright, G., Sidibe, M., & Akinsanola, A. (2020). Model uncertainties in climate change impacts on Sahel precipitation in ensemble of CMIP5 and CMIP6 simulations. *Climate Dynamics*, 55(5-6), 1385–1401. <https://doi.org/10.1007/s00382-020-05332-0>
- Moss, R. H., Edmonds, J. A., Hibbard, K. A., Manning, M. R., Rose, S. K., van Vuuren, D. P., et al. (2010). The next generation of scenarios for climate change research and assessment. *Nature*, 463(7282), 747–756. <https://doi.org/10.1038/nature08823>
- Oueslati, B., Bony, S., Risi, C., & Dufresne, J. (2016). Interpreting the inter-model spread in regional precipitation projections in the tropics: Role of surface evaporation and cloud radiative effects. *Climate Dynamics*, 47(9-10), 2801–2815. <https://doi.org/10.1007/s00382-016-2998-6>
- Park, J.-Y., Bader, J., & Matei, D. (2015). Northern-hemispheric differential warming is the key to understanding the discrepancies in the projected Sahel rainfall. *Nature Communications*, 6, 5985. <https://doi.org/10.1038/ncomms6985>
- Philander, S. G. H., Gu, D., Lambert, G., Li, T., Halpern, D., Lau, N.-C., & Pacanowski, R. C. (1996). Why the ITCZ is mostly north of the equator. *Journal of Climate*, 9(12), 2958–2972. [https://doi.org/10.1175/1520-0442\(1996\)009<2958:WTIIMN>2.0.CO;2](https://doi.org/10.1175/1520-0442(1996)009<2958:WTIIMN>2.0.CO;2)
- Rowell, D. P., & Chadwick, R. (2018). Causes of the uncertainty in projections of tropical terrestrial rainfall change: East Africa. *Journal of Climate*, 31(15), 5977–5995. <https://doi.org/10.1175/JCLI-D-17-0830.1>
- Schneider, T., Bischoff, T., & Haug, G. H. (2014). Migrations and dynamics of the intertropical convergence zone. *Nature*, 513(7516), 45–53. <https://doi.org/10.1038/nature13636>
- Trenberth, K. E., Stepaniak, D. P., & Caron, J. M. (2000). The global monsoon as seen through the divergent atmospheric circulation. *Journal of Climate*, 13(22), 3969–3993. [https://doi.org/10.1175/1520-0442\(2000\)013<3969:TGMAST>2.0.CO;2](https://doi.org/10.1175/1520-0442(2000)013<3969:TGMAST>2.0.CO;2)
- Wang, B., & Ding, Q. (2006). Changes in global monsoon precipitation over the past 56 years. *Geophysical Research Letters*, 33, L06711. <https://doi.org/10.1029/2005GL025347>
- Wang, B., & Ding, Q. (2008). Global monsoon: Dominant mode of annual variation in the tropics. *Dynamics of Atmospheres and Oceans*, 44(3-4), 165–183. <https://doi.org/10.1016/j.dynatmoc.2007.05.002>
- Wang, B., Jin, C., & Liu, J. (2020). Understanding future change of global monsoons projected by CMIP6 models. *Journal of Climate*, 33(15), 6471–6489. <https://doi.org/10.1175/JCLI-D-19-0993.1>
- Wang, B., Li, J., Cane, M. A., Liu, J., Webster, P. J., Xiang, B., et al. (2018). Toward predicting changes in the land monsoon rainfall a decade in advance. *Journal of Climate*, 31(7), 2699–2714. <https://doi.org/10.1175/JCLI-D-17-0521.1>
- Wang, B., Liu, J., Kim, H. J., Webster, P. J., & Yim, S. Y. (2012). Recent change of the global monsoon precipitation (1979–2008). *Climate Dynamics*, 39(5), 1123–1135. <https://doi.org/10.1007/s00382-011-1266-z>
- Wang, B., Liu, J., Kim, H. J., Webster, P. J., Yim, S. Y., & Xiang, B. (2013). Northern Hemisphere summer monsoon intensified by mega-El Niño/Southern Oscillation and Atlantic Multidecadal Oscillation. *Proceedings of the National Academy of Sciences of the United States of America*, 110(14), 5347–5352. <https://doi.org/10.1073/pnas.1219405110>
- Wang, P., Wang, B., Cheng, H., Fasullo, J., Guo, Z. T., Kiefer, T., & Liu, Z. Y. (2014). The global monsoon across time scales: Is there coherent variability of regional monsoons? *Climate of the Past Discussions*, 10(3), 2163–2291. <https://doi.org/10.5194/cpd-10-2163-2014>
- Wang, P., Wang, B., Cheng, H., Fasullo, J., Guo, Z. T., Kiefer, T., & Liu, Z. Y. (2017). The global monsoon across time scales: Mechanisms and outstanding issues. *Earth-Science Reviews*, 174, 84–121. <https://doi.org/10.1016/j.earscirev.2017.07.006>
- Webster, P. J. (1987). The elementary monsoon. In J. S. Fein, & P. L. Stephens (Eds.), *Monsoons* (pp. 3–32). New York, NY: John Wiley.
- Webster, P. J., & Yang, S. (1992). Monsoon and ENSO: Selectively interactive systems. *Quarterly Journal of the Royal Meteorological Society*, 118(507), 877–926. <https://doi.org/10.1002/qj.49711850705>
- Xiang, B., Zhao, M., Ming, Y., Yu, W., & Kang, S. (2018). Contrasting impacts of radiative forcing in the Southern Ocean versus southern tropics on ITCZ position and energy transport in one GFDL climate model. *Journal of Climate*, 31(14), 5609–5628. <https://doi.org/10.1175/JCLI-D-17-0566.1>
- Xie, P., & Arkin, P. A. (1997). Global precipitation: A 17-year monthly analysis based on gauge observations, satellite estimates, and numerical model outputs. *Bulletin of the American Meteorological Society*, 78(11), 2539–2558. [https://doi.org/10.1175/1520-0477\(1997\)078<2539:GPAYMA>2.0.CO;2](https://doi.org/10.1175/1520-0477(1997)078<2539:GPAYMA>2.0.CO;2)
- Xie, S., Deser, C., Vecchi, G., Collins, M., Delworth, T. L., Hall, A., et al. (2015). Towards predictive understanding of regional climate change. *Nature Climate Change*, 5(10), 921–930. <https://doi.org/10.1038/nclimate2689>
- Zhou, T., Yu, R., Li, H., & Wang, B. (2008). Ocean forcing to changes in global monsoon precipitation over the recent half-century. *Journal of Climate*, 21(15), 3833–3852. <https://doi.org/10.1175/2008JCLI2067.1>